Proceedings of the 7th World Congress on Momentum, Heat and Mass Transfer (MHMT'22)
~~Lisbon, Portugal~~ Virtual Conference – April 19-22, 2022
Paper No. ENFHT 193
DOI: 10.11159.enfht22.193

Experimental Investigation of the Interaction of Axial Transport and Drying in Rotary Kilns

Claudia Meitzner[1], Fabian Herz[2], Eckehard Specht[1], Bilal Mehdi[1], Jakob Seidenbecher[1],
[1]Otto von Guericke University Magdeburg, Institute of Fluid Dynamics and Thermodynamics,
Universitätsplatz 2, 39106 Magdeburg, Germany
claudia.meitzner@ovgu.de; bilal.mehdi@ovgu.de; eckehard.specht@ovgu.de
[2]Anhalt University of Applied Sciences, Applied Biosciences and Process Engineering,
Bernburger Str. 55, 06366 Köthen, Germany
fabian.herz@hs-anhalt.de

Abstract **-** Rotary kilns are used for the thermal treatment of various bulk materials and part of different sectors of industry, where also drying processes play a vital role. The drying process is mainly affected by the temperature of the particles inside the packed bed. This temperature is influenced by the heat transfer on the one hand and on the axial and transversal motion dynamics of the particles on the other hand.
To investigate the phenomenological interactions of the heat transfer mechanisms as well as the drying effect and the axial transport, an indirectly heated pilot rotary kiln was designed (D = 0.5 m; L = 1.76 m). Sensitive thermocouples of type K 0.5 mm are used to measure the temperatures inside the kiln. Therefore, a strut profile with connected precision pipes is used to lead a total of 32 thermocouples to different transversal and axial position. As this measuring system is mounted at the rotating kiln wall, the thermocouples rotate together with the kiln and are therefore able to record the radial and axial temperature distribution. Depending on their positions inside the kiln, the thermocouples measure the temperatures of the bulk bed, gas phase and kiln wall, respectively.
Additionally, at different axial positions, samples were taken out of the bulk bed and the moisture content of those samples were determined using a thermo-gravimetric analysis.
In this way, continuous experiments were taken out using expanded clay as testing material. Varying the rotational speed and the mass flow rate, the influence of these parameters on the drying process is analyzed.

Keywords**:** Rotary Kiln, Drying Process, Axial Transport, Residence Time

1. Introduction

Rotary kilns are employed for various industrial processes like calcination, reduction or dehydration, where drying is a primary process. Rotary kilns mainly consist of a cylindrical drum which is inclined slightly to the horizontal and rotates around its own axis. On the upper end of the drum, granular material is fed, so that it moves through the kiln due to inclination and rotation. Depending on the set parameters, an axial bed profile forms and a specific residence time of the particles occurs. The transport of the bulk bed is dependent of both, the transverse and the axial movement of the particles, as they overlap and cause the final path the single particles take inside the bulk bed.

Mellmann [1] and Henein [2], [3] investigated the transverse motion in rotary kilns in detail by characterizing different types of motion which depend on the parameters filling degree, rotational speed and friction coefficients. Additionally, the axial motion has to be considered, as it mainly influences the residence time of the particles. The axial material movement can mainly be described by continuum models like i.e. from [4]. How the axial bed profile develops, influences the contact areas through which the heat transfer takes place. Therefore, it is important to know the occurring free and covered bed surfaces.

The heat transfer mechanism in indirectly heated rotary kilns was experimentally investigated by Nafsun and Herz [5], [6]. It was found that the contact heat transfer between bulk bed and inner drum wall was dominating. Additionally, they studied the mixing behaviour [7], [8] and Herz developed a mathematical process model [9] to simulate thermal processes in rotary kilns in which the drying process was not included.

Drying processes in rotating cylinders have been investigated mainly for specific applications i.e. to dry chilli [10] or peppermint [11] or when the rotary drums consists of porous walls [12] or have flights included [13].

Finally, it can be said, that a lot of research has been done in the general field, but a detailed investigation of the interaction of the simultaneously running mechanisms such as material motion, heat transfer and drying process has not been observed so far. The present analysis shows the drying process in indirectly heated rotary kilns during axial transport.

2. Test Material and Experimental Setup

2.1. Test Material

Expanded clay was identified as test material to investigate the drying process in a pilot rotary kiln as the material can easily be wetted, dried and reused for further experiments, without changing its properties. Therefore, three particle fractions were classified as 1-3, 3-5 and 5-8 mm, respectively, see Fig. 1 and were separated through a sieving process.

a) b) c)

Fig. 1: Expanded clay of 1-3 mm (a), 3-5 mm (b) and 5-8 mm (c).

Using DIN ISO 697 and EN ISO 60, the bulk density was determined, see Table 1.

Table 1: Material properties of expanded clay.

	Particle diameter fraction [mm]	Bulk density ρ_S [kg/m^3]	Dynamic angle of repose θ [°]
dry material	1-3	1003 ± 5	34
	3-5	831 ± 3	33
	5-8	676 ± 6	32
wet material	1-3	1029 ± 16	37
	3-5	845 ± 3	39
	5-8	687 ± 5	32

To investigate the transverse motion of the material, it was studied in a batch rotary drum (D = 0.5 m, L = 0.15 m). The inner drum consists of the same material as the pilot rotary kiln which was used for the drying analysis, to assure the same wall surface conditions. The drum was mounted onto a gear motor and the front side was closed with a glass plate to make the transverse motion visible, see Fig. 2, a).

Fig. 2: Experimental setup to investigate the transverse motion (a) and dynamic angle geometry (b).

By varying the filling degree and the rotational speed, for each condition, the occurring motion type as well as the dynamic angle of repose θ could be identified, see Fig. 2 b). The results are shown in Tab. 1 as well.

2.2. Experimental Setup

Continuous experiments were taken out at an indirectly heated rotary kiln with a diameter of D = 0.5 m and a total length of L = 1.76 m, see Fig. 3.

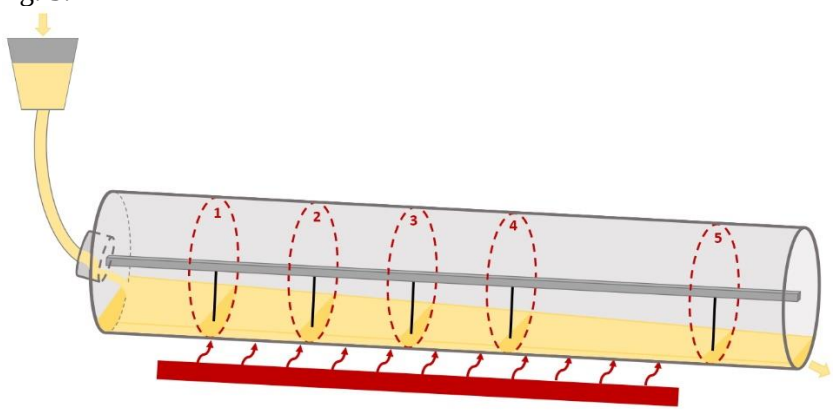

Fig. 3: Experimental setup to investigate the heat transfer and drying process.

Before starting the experiment, the test material was wetted in a water bath for several hours and surplus water was let dropped down afterwards. Then, the material was filled into a feeder, which was positioned above the upper side of the rotary kiln. The slope angle β was adjusted and the empty pilot kiln was heated up to the desired heating temperature T_{Heat}. Then, the material was fed with a certain mass flow rate $\dot{M}$. The time to achieve the steady state (constant bed profile and temperature distribution) depends on the rotational speed n and the other set parameters. As soon as the steady state was achieved, the temperature measurement was started. By using 0.5 mm sensitive thermocouples of type K, the temperature data at five axial positions was recorded. Therefore, a strut profile was attached at the middle axe of the kiln and was mounted at the inner kiln wall so that it rotates together with the kiln. At this strut profile, thermocouples were installed at different radial positions. As a result, the thermocouples measure both, the air and the solid bed temperature depending on their time dependent position, see Fig. 4.

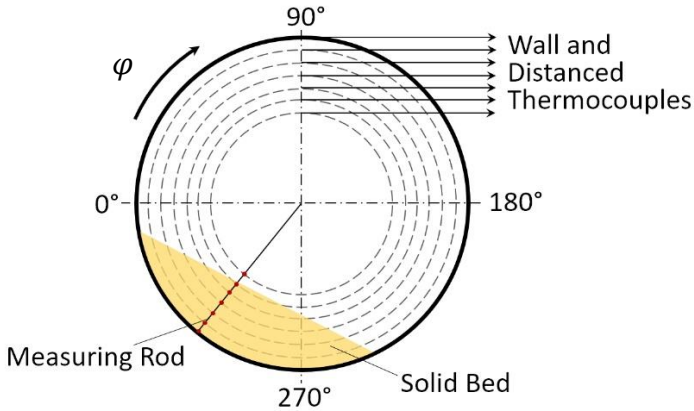

Fig. 4: Thermocouple arrangement in the cross section of the pilot rotary kiln.

Additionally, at each axial position, one thermocouple was also fixed at the wall to measure the wall temperature. To allocate the temperatures with the position at which they were measured, the corresponding circumferential angle of the measuring rod is recorded. The circumferential angle φ is defined like shown in Figure 4, where the 0° value starts at the 9 o'clock position and increases with the rotation, clockwise. The data containing time, circumferential angle and temperatures of all thermocouples was transferred wireless to a computer, where it is saved as a .txt file.

To identify the drying progress depending on the length of the kiln, samples were taken out of the solid bed at the previously defined axial positions. Those samples were analyzed thermo-gravimetrically using a TGA701 (LECO).

3. Analyzing Method

3.1. Axial Motion

Depending on the set parameters, an axial bed profile was developed. The bed heights at the axial positions could be detected with the help of a video analysis and were illustrated using a MatLab program, see Fig. 5.

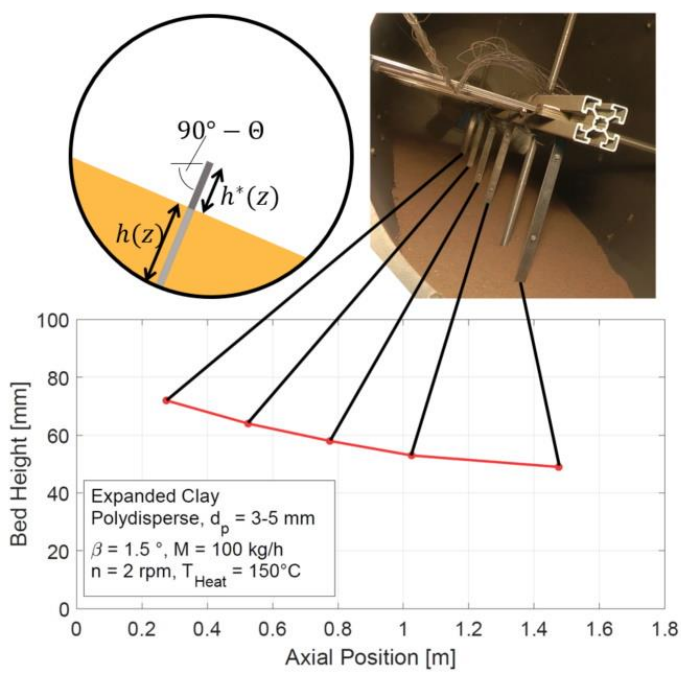

Fig. 5: Axial bed height profile.

Therefore, the visible part of a steel ruler H^* was measured in pixels with image analysis tool ImageJ. By knowing the total length of the ruler in pixels H_0 as well as the total length of the ruler in mm h_0, the real bed height h_z can be calculated for each axial position z

$$h_z = h_0 \left(1 - \frac{H^*}{H_0}\right). \tag{1}$$

3.2. Temperature Distribution

The thermocouples measure the temperatures in axial, transverse and radial direction so that wall, solid and air temperatures are known. Fig. 6 illustrates the circumferential temperature profile at the middle position for one reference experiment during steady state.

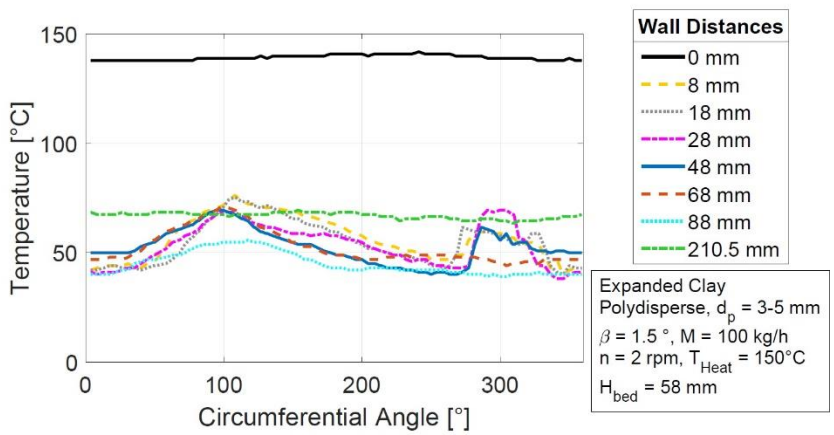

Fig. 6: Circumferential temperature profile at the middle position.

As the pilot rotary kiln was heated indirectly, the wall temperature shows the highest values all the time. For the respective experiment, a maximal bed height of 58 mm was observed from the video analysis. Thus, all thermocouples with a wall distance smaller than 58 mm immerse into the solid bed in the range of a circumferential angle of 270 to 320 °. As soon as the solid bed temperature is measured, a temperature increase can be remarked.

By knowing the bed heights and the dynamic angle of repose, it can be clearly seen which measurements are solid or air temperatures. Afterwards mean temperatures were calculated to show the axial temperature development of wall, solid and air, see Fig. 7.

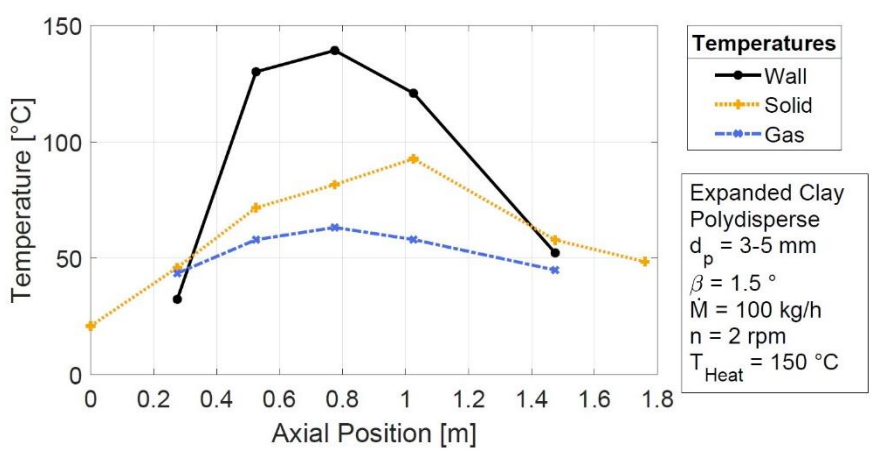

Fig. 7: Axial temperature profile.

Because the heater was positioned in the middle zone only, the wall temperatures at the inlet and outlet sides are obviously smaller. The material was fed with ambient temperature and was heated through radiation of the hot walls on the free bed surface and through contact heat transfer from the wall to the solids. It can be seen, that the material heats up faster at the beginning, slower in the middle zone. The temperature difference of wall and solids is the driving force for this heat transfer and it reduces in this region.

3.3. Drying Procedure

To investigate the axial drying proceeding, samples were taken out of the solid bed, at the different axial positions, where also the temperatures are measured. As the initial moisture content varied within the different experiments, a normalized moisture content in percent was used for analysis, using the following equation

$$\bar{X} = 100 - \left(\frac{X - X_0}{X_0}\right) \cdot 100 \tag{2}$$

where X is the moisture content of the respective position and X_0 is the initial moisture content, respectively.

The moisture content as well as the normalized moisture content are illustrated over the axial kiln length, see Fig. 8.

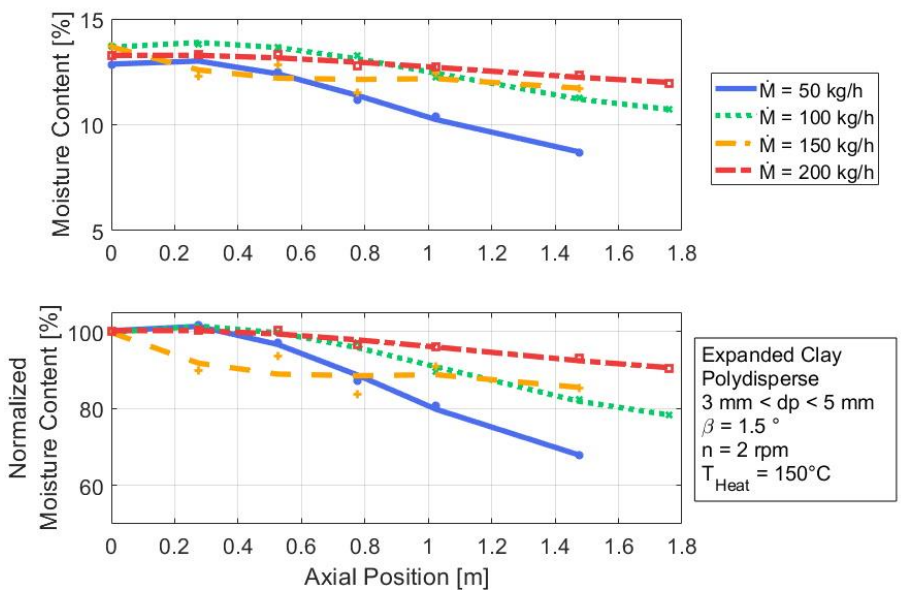

Fig. 8: Moisture content and Normalized moisture content over axial length.

A drying rate is calculated by investigating the maximal drying progress respecting

$$d\bar{X} = \left|\frac{\bar{X}_{end} - \bar{X}_0}{z_{end} - z_0}\right| \tag{3}$$

where the total change of the normalized moisture content is considered from the initial moisture $\bar{X}_0(z_0 = 0)$ to the moisture content at the end position of the kiln $X_{end}(z_{end})$.

By comparing the drying rate of different experiments, the influence of the variated parameters can be seen.

Fig. 9 shows the repeatability of the experiments and the determined drying rate.

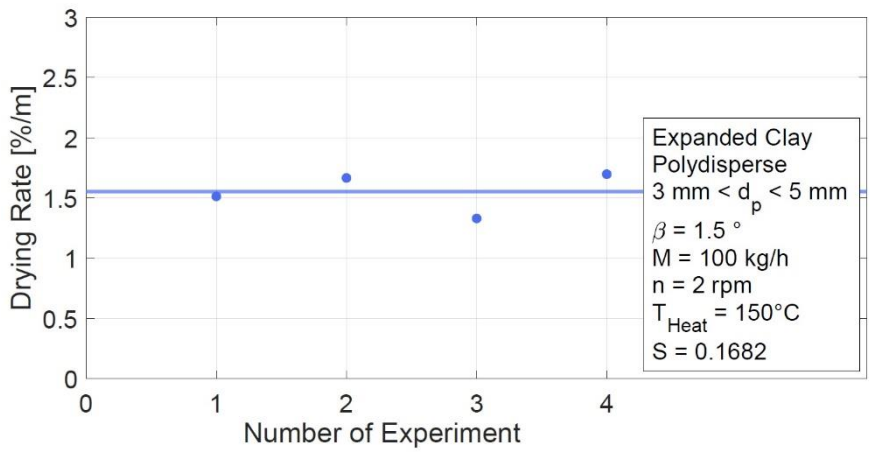

Fig. 9: Influence of mass flow rate on the drying rate.

Four experiments with the exact same conditions were done to prove the accuracy of the experimental work and the determination of the target value using the described procedure. It is obvious, that the drying rate varies very slightly. The standard deviation is S = 0.1682.

Fig. 10 shows the influence of the mass flow rate on the drying rate.

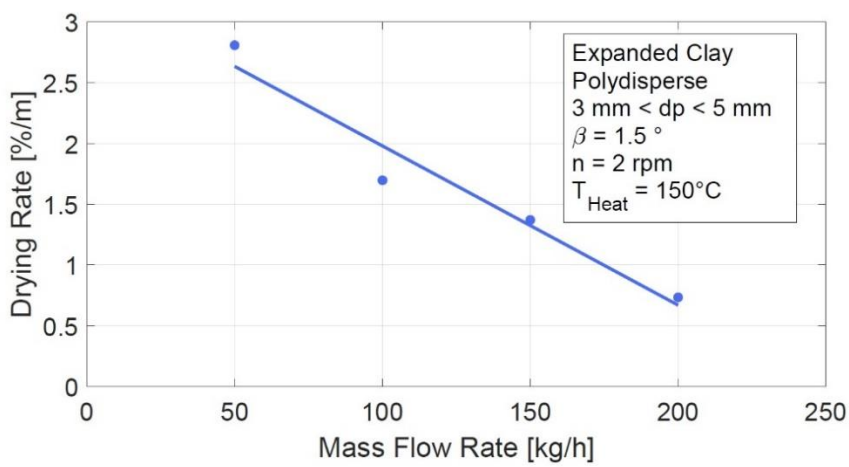

Fig. 10: Influence of mass flow rate on the drying rate.

It can be seen, that for less mass flow rates, the drying effect is higher. Less material is moving through the kiln but the provided heat remains the same. By increasing the mass flow rate, the drying rate reduces, as more material needs more heat to let the water evaporate.

The effect of the rotational speed is illustrated in Fig. 11.

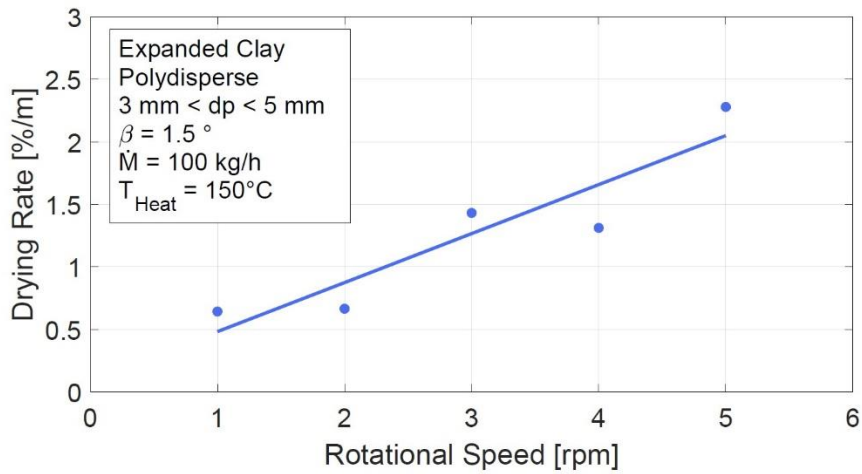

Fig. 11: Influence of rotational speed on the drying rate.

A lower rotational speed causes a lower drying rate. With an increase of the rotational speed, the drying rate increases as well. The evaporation mainly occurs at the free surface of the solid bed, because there the moisture can easily pass into the gas phase. By increasing the rotational speed, the transverse material movement is increased and therefore the mixing is improved which leads to a more intensive contact of particles and gas phase and increases the evaporation.

4. Conclusion

To investigate the drying process of bulk materials in rotary kilns, experiments have been done. On the basis on the total drying progress, a drying rate was calculated to analyze the influence of the varied parameters mass flow rate of material and rotational speed. Higher mass flow rates cause a decrease in drying rate. The drying rate improves by increasing the rotational speed, because of a more intensive gas-solid contact and a better mixing.

Further investigations of the continuous drying process are planned to study the influence of particle size, inclination angle and heating temperature.

Nomenclature

Symbol	Description	Unit
$\boldsymbol{D}$	Diameter of the pilot rotary kiln	m
$\boldsymbol{d\bar{X}}$	Drying rate	%/m
$\boldsymbol{d_P}$	Particle diameter	mm
$\boldsymbol{H_0}$	Total length of steel ruler	px
$\boldsymbol{H^*}$	Visible part of steel ruler	px
$\boldsymbol{h_0}$	Total length of steel ruler	mm
$\boldsymbol{h_z}$	Bed height at position z	mm
$\boldsymbol{L}$	Length of the pilot rotary kiln	m
$\boldsymbol{\dot{M}}$	Mass flow rate	kg/h
$\boldsymbol{n}$	Rotational speed	rpm

Symbol	Description	Unit
$\boldsymbol{T}$	Temperature	°C
$\boldsymbol{X}$	Moisture content	%
$\boldsymbol{X_0}$	Initial moisture content	%
$\boldsymbol{X_{end}}$	Final moisture content	%
$\boldsymbol{\bar{X}}$	Normalized moisture content	%
$\boldsymbol{z}$	Length of the pilot rotary kiln	m
$\boldsymbol{\beta}$	Inclination angle of the kiln	°
$\boldsymbol{\theta}$	Dynamic angle of repose	°
$\boldsymbol{\rho_S}$	Bulk density of the solids	kg/m^3
$\boldsymbol{\varphi}$	Circumferential angle	°

References

[1] J. Mellmann, "The transverse motion of solids in rotating cylinders—forms of motion and transition behavior," *Powder Technology*, vol. 118, no. 3, pp. 251–270, 2001, doi: 10.1016/S0032-5910(00)00402-2.

[2] H. Henein, J. K. Brimacombe, and A. P. Watkinson, "Experimental Study of Transverse Bed Motion in Rotary Kilns," *Metallurgical Transactions B*, pp. 191–205, 1983.

[3] M. Henein, J. K. Brimacombe, and A. P. Watkinson, "The modeling of transverse solids motion in rotary kilns,"

[4] P. F. Britton, M. E. Sheehan, and P. A. Schneider, "A physical description of solids transport in flighted rotary dryers," *Powder Technology*, vol. 165, no. 3, pp. 153–160, 2006, doi: 10.1016/j.powtec.2006.04.006.

[5] A. I. Nafsun, F. Herz, E. Specht, V. Scherer, and S. Wirtz, "THE CONTACT HEAT TRANSFER IN ROTARY KILNS AND THE EFFECT OF MATERIAL PROPERTIES," *10th International Conference on Heat Transfer, Fluid Mechanics and Thermodynamics*, 2014.

[6] F. Herz, I. Mitov, E. Specht, and R. Stanev, "Influence of operational parameters and material properties on the contact heat transfer in rotary kilns," *International Journal of Heat and Mass Transfer*, vol. 55, 25-26, pp. 7941–7948, 2012, doi: 10.1016/j.ijheatmasstransfer.2012.08.022.

[7] A. I. Nafsun F. Herz, E. Specht, H. Komossa, S. Wirtz, V. Scherer, X. Liu., "Thermal bed mixing in rotary drums for different operational parameters," *Chemical Engineering Science*, vol. 160, pp. 346–353, 2017, doi: 10.1016/j.ces.2016.11.005.

[8] A. I. Nafsun, F. Herz, E. Specht, H. Komossa, S. Wirtz, and V. Scherer, "EXPERIMENTAL INVESTIGATION OF THERMAL BED MIXING IN ROTARY DRUMS," *11th International Conference on Heat Transfer, Fluid Mechanics and Thermodynamics*, 2015.

[9] F. Herz, *Entwicklung eines mathematischen Modells zur Simulation thermischer Prozesse in Drehrohröfen*. Doktorarbeit, 2012.

[10] W. Kaensup, S. Chutima, and S. Wongwises, "EXPERIMENTAL STUDY ON DRYING OF CHILLI IN A COMBINED MICROWAVE-VACUUM-ROTARY DRUM DRYER," *Drying Technology*, vol. 20, no. 10, pp. 2067–2079, 2002, doi: 10.1081/DRT-120015585.

[11] S. Tarhan, İ. Telci, M. T. Tuncay, and H. Polatci, "Product quality and energy consumption when drying peppermint by rotary drum dryer," *Industrial Crops and Products*, vol. 32, no. 3, pp. 420–427, 2010, doi: 10.1016/j.indcrop.2010.06.003.

[12] H. Didriksen, "Model based predictive control of a rotary dryer," *Chemical Engineering Journal*, vol. 86, 1-2, pp. 53–60, 2002, doi: 10.1016/S1385-8947(01)00272-8.

[13] M. H. Lisboa, D. S. Vitorino, W. B. Delaiba, J. R. D. Finzer, and M.A.S. Barrozo, "A STUDY OF PARTICLE MOTION IN ROTARY DRYER," *Brazilian Journal of Chemical Engineering*, 24-3, pp. 365–374, 2007.